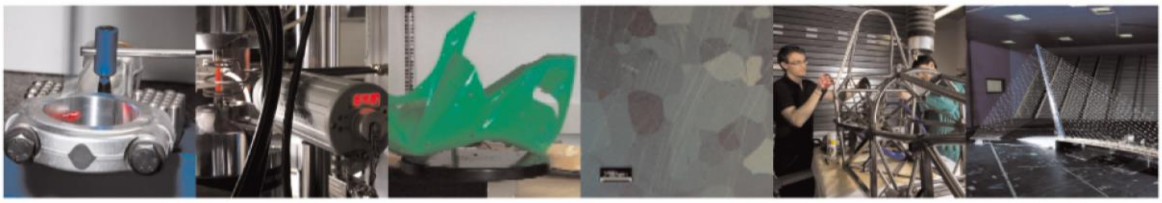

Continuous multi-angle variation (CMAV) for faster roundness correction in centreless grinding

Hossein Safarzadeh, Michele Monno

This is a post-peer-review, pre-copyedit version of an article published in The International Journal of Advanced Manufacturing Technology. The final authenticated version is available online at: http://dx.doi.org/10.1007/s00170-021-08647-2

DIPARTIMENTO DI MECCANICA ■ POLITECNICO DI MILANO
via G. La Masa, 1 ■ 20156 Milano ■ EMAIL (PEC): pecmecc@cert.polimi.it
http://www.mecc.polimi.it
Rev. 0

Continuous Multi Angle Variation (CMAV) For Faster Roundness Correction in Centerless Grinding

Hossein Safarzadeh[a,*], *Michele Monno*[a]

[a]*Politecnico di Milano, Dipartimento di Meccanica, Via Giuseppe La Masa, 1, 20156 Milano, Italy*

* Corresponding author. *E-mail address:* hossein.safarzadeh@polimi.it

---

Abstract

This paper presents a new methodology to improve roundness process of the centerless grinding based on classic stability diagrams and relative rounding mechanism. This study shown that, it is not always convenient to have a fixed setup angle. Based on simulation results it is suggested to consider the raw workpiece profile before selection these parameters accordingly to the type of raw workpiece roundness error (odd or even lobed). It was found that changing the setup angles from an initial appropriate point to a final point, results in better simulated and experimented roundness. This changing was simulated with two methods, continuous and multistep but the best results was achieved by first one. Furthermore, a new support blade design for through feed centerless grinding is presented for application of above-mentioned method.

Keywords: Centerless grinding; Through feed, Geometrical stability, Roundness correction, Continuous multi angle variation

---

1. Introduction

As Dhavlikar et al [1] describes Centerless grinding is a common manufacturing grinding process for round work-pieces, thanks to its unique work-piece (WP) holding system. The WP is sustained along three contact lines, with the grinding wheel, the regulating wheel, and the supporting blade (*Figure 1*). This method removes the need to clamp the workpiece and create centering holes on the workpiece. WP loading and unloading is easier, which results in reduced cycle time and higher productivity. Nevertheless, Zhou et al [2] mentions due to this setup, centerless grinding is exposed to roundness errors generated by two types of instabilities: dynamic regenerative chatter and geometric lobing. Dynamic chatter, due to the interaction between the cutting process and the main resonances of the machine structure, is a very usual phenomenon in machining processes. Gallego [3] defines the Geometric lobing, as product of the peculiar geometric setup of the WP, i.e., blade angle and WP height. As Klocke [4] shows in his study, it's one of the main constraints to WP roundness accuracy: WP center can oscillate, provoking an irregular material removal which in turn increases WP waviness.

Dall [5] conducted the first significant research on the out-of-roundness WP problem, systematically relating the roundness error to the geometric configuration. Two main parameters were considered: the tangent angle and the top supporting blade angle. Then Yonetsu [6] defined the interactions between pre and post grinding amplitudes of harmonics of the WP profile. And Rowe et al [7] simulated the centerless grinding lobing problem on a digital computer taking into account all previous geometrical contemplations and presented the analytical model of the so-called *geometric rounding mechanism*. Later Marinescu et al [8] used these results to explain the geometric roundness error regeneration process. After describing the basic geometrical connections of the process, it was possible to use different stability criteria, like Nyquist criterion, to show the theoretical instabilities produced by different configurations. Various researchers such as Bueno et al [9] claimed that it is possible to create a stability map using the Nyquist criterion for each possible number of complete undulations that can be generated on the WP . Zhou et al [2] presented the periodic characteristic roots distribution of the lobing loop and recommended a nominal stability diagram to suggest the range of the center-height angle in order to lessen the lobing effect. Rowe et al [10,11] introduced the geometric stability parameter derived from the Nyquist stability criterion, limited to integer lobes. Furthermore, Qi cui et al [12] have developed a workpiece dynamics model by incorporating the geometric motion to represent the movements of the workpiece, grinding wheel and control wheel. This model can be used to analyze the workpiece rounding process and predict its roundness errors. Using these bases, Bianchi et al [13] considered the nonlinearity due to the loss of contact under large waviness, investigating its effect on process stability. Consequently, by calculating stability parameter for different combinations of geometric setup it is possible to obtain a general stability map (*Figure 2*) in order to find stable zones and prevent any unwanted geometric instabilities [14].

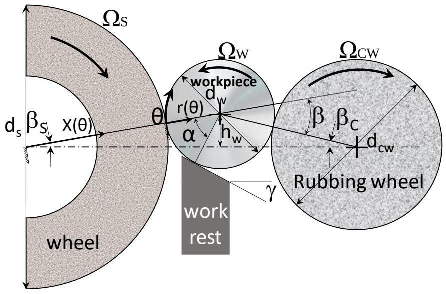

Figure 1: Centreless grinding geometry

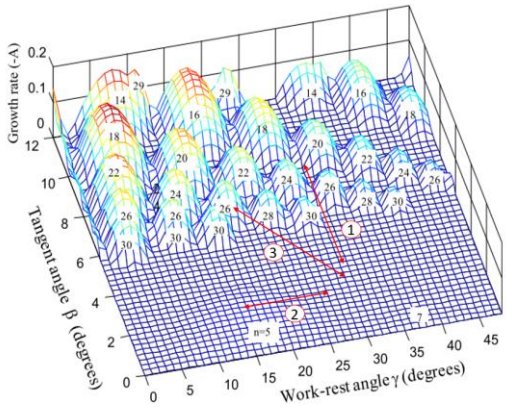

Figure 2: Stability map [14]

2. Geometric Stability Diagram

Nevertheless, the above-mentioned method, founded on stability maps for the process configuration, introduces various disadvantages [15]:

a) Due to other instability conditions (spinning, flat bad & etc.) it could be difficult to select some stable area.
b) The level of stability ("negative growth rate") implies the ability of achieving a good roundness by eliminating the geometric error already expound on the raw workpiece and since best growth rates are only slightly negative, hence the smoothing process is rather slow.

And some few points are worth to be mentioned:

a) At small values of β, only odd-lobed growth will occur, and then only at small rates.
b) At big values of β, only even-lobed growth will occur.
c) At small values of β (0°-5°), with Ɣ = 0°, 30° or 45°, no lobes are predicted to grow

Machine manufacturers based on their field experience usually suggest a setting with Ɣ=30° and β=7°. Nevertheless, for small values of β, the levels of lobes degeneration are very slow. In some cases, the initial workpiece profile has defects due to a previous manufacturing process such as bar extrusion that creates a consistent profile along the bar, or a machining process (e.g., roughing by another centerless grinding) that creates specific number of the lobes due to the process geometric setup. Thus, if a previous manufacturing process has left an odd-lobed profile (3,5,7, etc.) or even-lobed profile (2,4,6, etc) on the piece, or even if the piece has a highly irregular surface which consequently includes many lobe frequencies and centreless grinding under these set-up conditions will only remove these lobes very gradually. To remove it quickly, β must be increased or decreased, so risking growth of other lobe numbers.

3. Continuous Multi Angle Variation (CMAV)

Several stable or nearly stable 'trails' across *Figure 2* are detectable. If {β & Ɣ} were altered in a synchronized manner along one of these trails during grinding, it would have potential to conquer the above problem of removing odd o even numbered lobes. For instance, for an even-lobed profiled workpiece is the best to initial the process in odd-lobing zone and finish it in a neutral zone or vice versa for an odd-lobed workpiece. Or, in case of high roughness as explained above is suggested to follow a path which contained all three zone with neutral zone at the end to eliminate randomly placed lobes.

For doing so, let us consider 3 different possible scenarios:

1. Keeping support blade angle Ɣ fixed and changing tangent angle β. As depicted in *Figure 1* this solution can be done by changing the height of centre of workpiece between the machining processes (roughing and finishing) (*Figure 2* (1)).
2. Keeping tangent angle β fixed and changing support blade angle Ɣ. this solution can be done by changing the inclination of support blade angel between the machining process (roughing and finishing) (*Figure 2* (2)).
3. Changing both support blade angle Ɣ and tangent angle β simultaneously (*Figure 2* (3)).

The first two scenarios are applicable in both plunge and through feed centreless grinding. Simply by dividing the production cycle into two cycles (multistep), roughing, and finishing and utilising two different support blades for each process or doing both process in a unique cycle (continuous) by changing WP height with an additional motorized axis (*Figure 3*) or using a profiled blade to change the angle β (*Figure 4*) [15]. However, the second approach is highly limited to the ratio between support blade thickness and WP diameter and results to be non-applicable for the most of small to medium diameters. However, last scenario in only applicable for through feed process since changing both angles simultaneously is physically and geometrically very difficult for plunge grinding process.

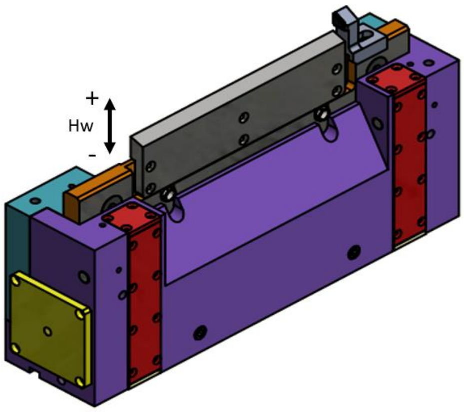

Figure 3: Automatic Support Blade

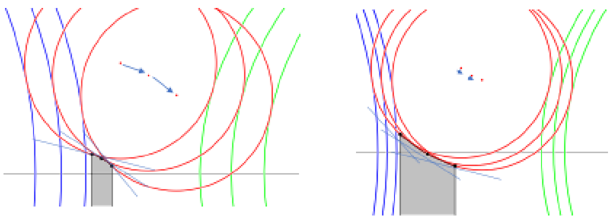

Figure 4: Profiled blade

Although, all three scenarios can be used in though feed centreless grinding and there is no need to divide the process, since workpiece passes through the machine (*Figure 5*) and gives the possibility to create a supporting blade that start with a specific set of β° and Ɣ° and finished with different set of β° and Ɣ° *Figure 6*. Producing the supporting blade with this hypothesis is very complicated and needs EDM process to be manufactured. Also, For achieving a workpiece with acceptable cylinder error, the truing of control wheel profile should be done with CAM software to guarantee the perfect contact line with workpiece.

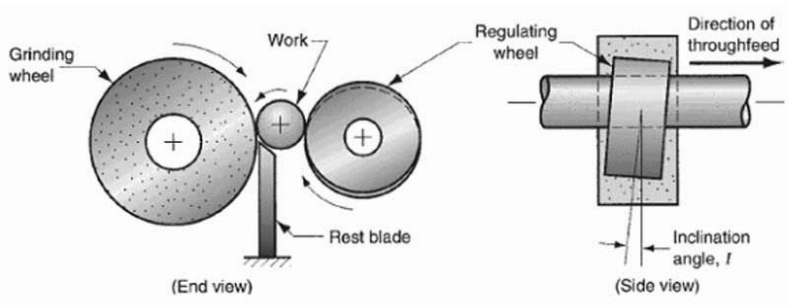

Figure 5: Through feed centreless grinding

For doing so, let consider Centreless rounding geometry as *Figure 1*, Angles α and β are related to work height and WR angle as follows:

$$\alpha = \frac{\pi}{2} - \Upsilon - \beta_s \qquad \text{Equation 1}$$

$$\beta = \beta_s + \beta_{cw} \qquad \text{Equation 2}$$

Where:

$$\beta_s = Sin^{-1}(\frac{2h_w}{d_s + d_w}) \qquad \text{Equation 3}$$

$$\beta_{cw} = Sin^{-1}(\frac{2h_w}{d_{cw} + d_w}) \qquad \text{Equation 4}$$

$$h_w = \frac{\beta}{2\left({}^{1}/{d_s + d_w} + {}^{1}/{d_{cw} + d_w}\right)} \qquad \text{Equation 5}$$

So, by introducing workpiece diameter (d_w), Grinding wheel diameter (d_s) and Control wheel diameter (d_{cw}) into *Equation 5* the height of centre of workpiece can be calculated for given β°.

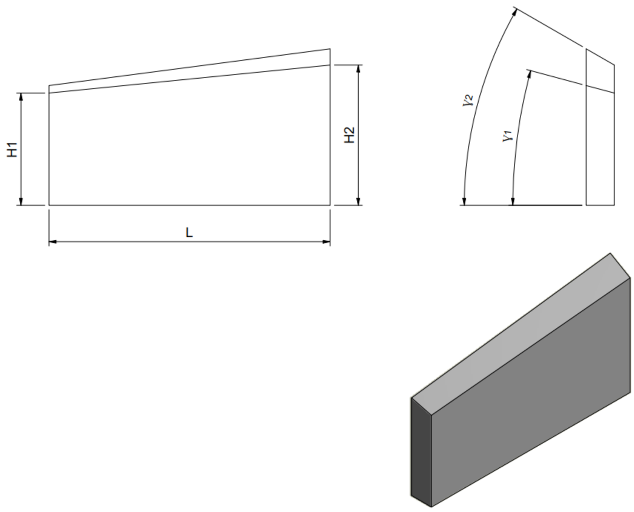

Figure 6: MTAV support blade

4. Simulations

In this section a series of roundness simulations are obtained base on a model proposed in [16]. The obtained process model is represented by the block diagram of *Figure 7*. Based on it, a numeric simulation code has been developed in Matlab™ to estimate the WP profile, discretized by a circular array of 7200 elements, representing WP radial reduction at a given angular position. The contact filtering has been implemented by a 0-phase symmetric FIR filter: a high order of 361 has been selected to fit properly the $Z_{cs}(n)$. Contact length l_{cs} has been computed and all the necessary parameters, such as R_r, $F_{n\prime}$, E_1, E_2, ν_1 and ν_2 have been taken from literature, given the WP material, and grinding wheel type and status. Stiffness factor K has been estimated fitting an exponential decay on wheel spindle current signal during spark-out tests.

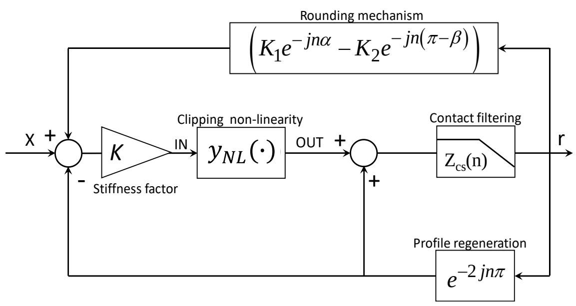

Figure 7. Model block diagram

The performance of the model is demonstrated through simulations of the grinding process in *Figure 8* & *Figure 9* simulating an initially rough component that has been ground for 100 rotations. The deviation error has been enlarged 2000 times to have clearer image of lobes created on workpieces and this causes a discontinuity on depicted simulated workpiece profile that can not be detected on real workpiece. *Figure 8* shows lobe amplitudes obtained using Ɣ= 30°, β = 8°, and *Figure 9* those for Ɣ=20°, β=1°. Comparing the simulated lobes number with those predicted from stability diagram *Figure 2: Stability mapFigure 2* with respected combination of Ɣ° and β° (Ɣ= 30°& β = 8° results in 20 lobes, Ɣ=20°, β=1° results in 5 lobes), it can be said that the model's results are acceptable.

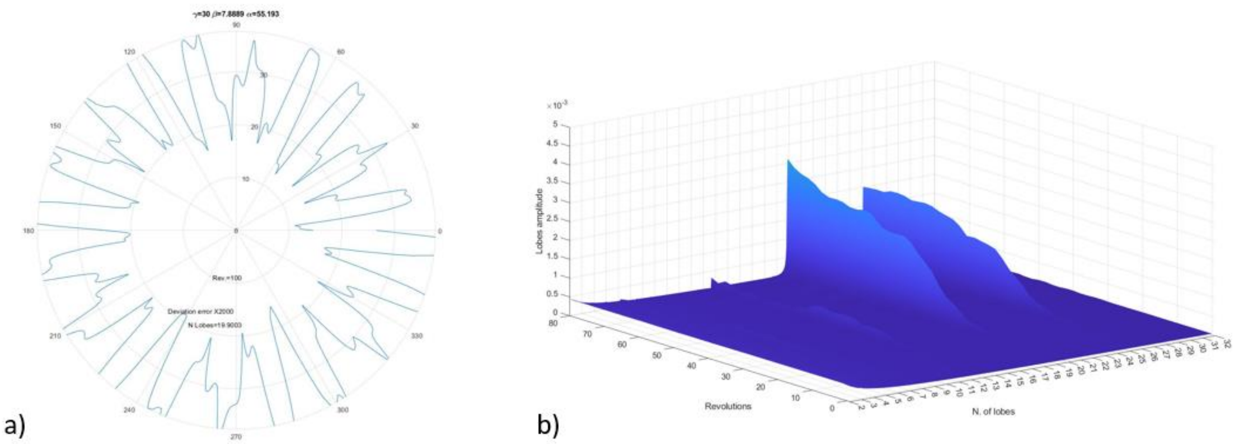

Figure 8: Ɣ= 30°, β = 8°, a) simulated profile, b) simulated lobes amplitude

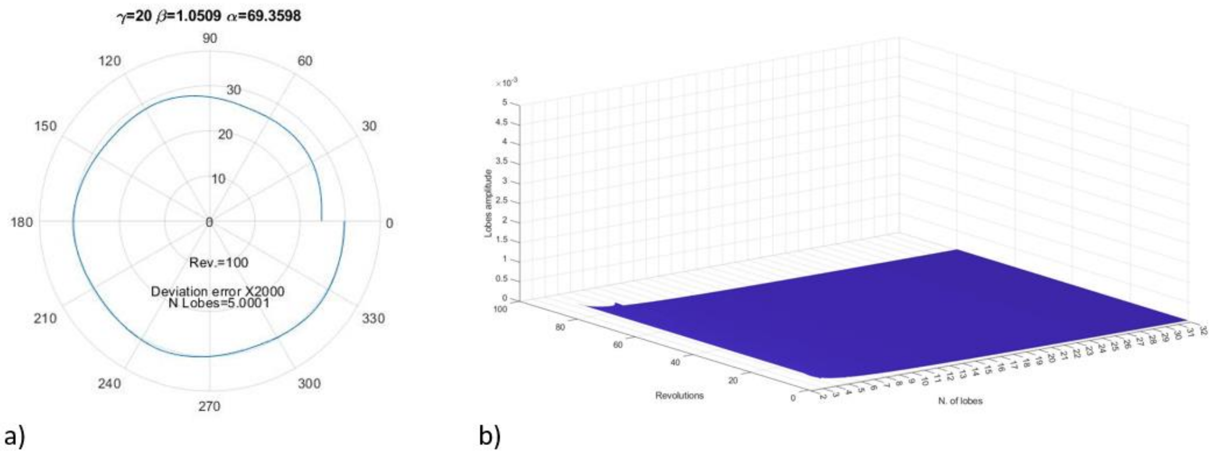

Figure 9: Ɣ= 20°, β = 1°, a) simulated profile, b) simulated lobes amplitude

For testing the hypothesis proposed in section 3, two different sets of simulations are considered based on two different raw profile of the workpieces. First set is based on grinding a workpiece with a 5 lobed raw profile (*Figure 10*) and second set is based on grinding a workpiece with a 6 lobed raw profile (Figure 15).

For grinding simulation of these workpieces four different conditions are considered:

1. Fixed β°=6.8° and Ɣ=30° (as suggested by numerous literatures[17]).
2. Varying both β° (Via Hw) and Ɣ°.
3. Varying β° with fixed Ɣ°.
4. Varying Ɣ° with fixed β°.

The variations speed in considered by : $\frac{\Delta \gamma}{\text{Number of revolutions}}$ and $\frac{\Delta \beta}{\text{Number of revolutions}}$

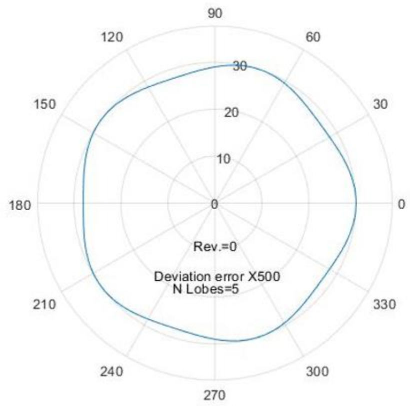

Figure 10: Raw workpiece with 5 lobes

In the conditions 2,3&4 two different methods are considered: continuous variation from initial point to the final point and process divided into two roughing and finishing (multistep) with 30% and 70% ratio of total workpiece revolutions in grinding process. As explained before the best condition for eliminating odd-lobed profile is best to select a zone from stability map which promises developments of an even-lobed profile for initial rounding process in other to accelerate the error elimination process and then select a neutral zone for finishing. Nevertheless, for an even-lobed profile, the initial rounding process should be located in a zone that potentially is favourable for developing odd-lobes and same as before it is the best to finish the process in a neutral zone.

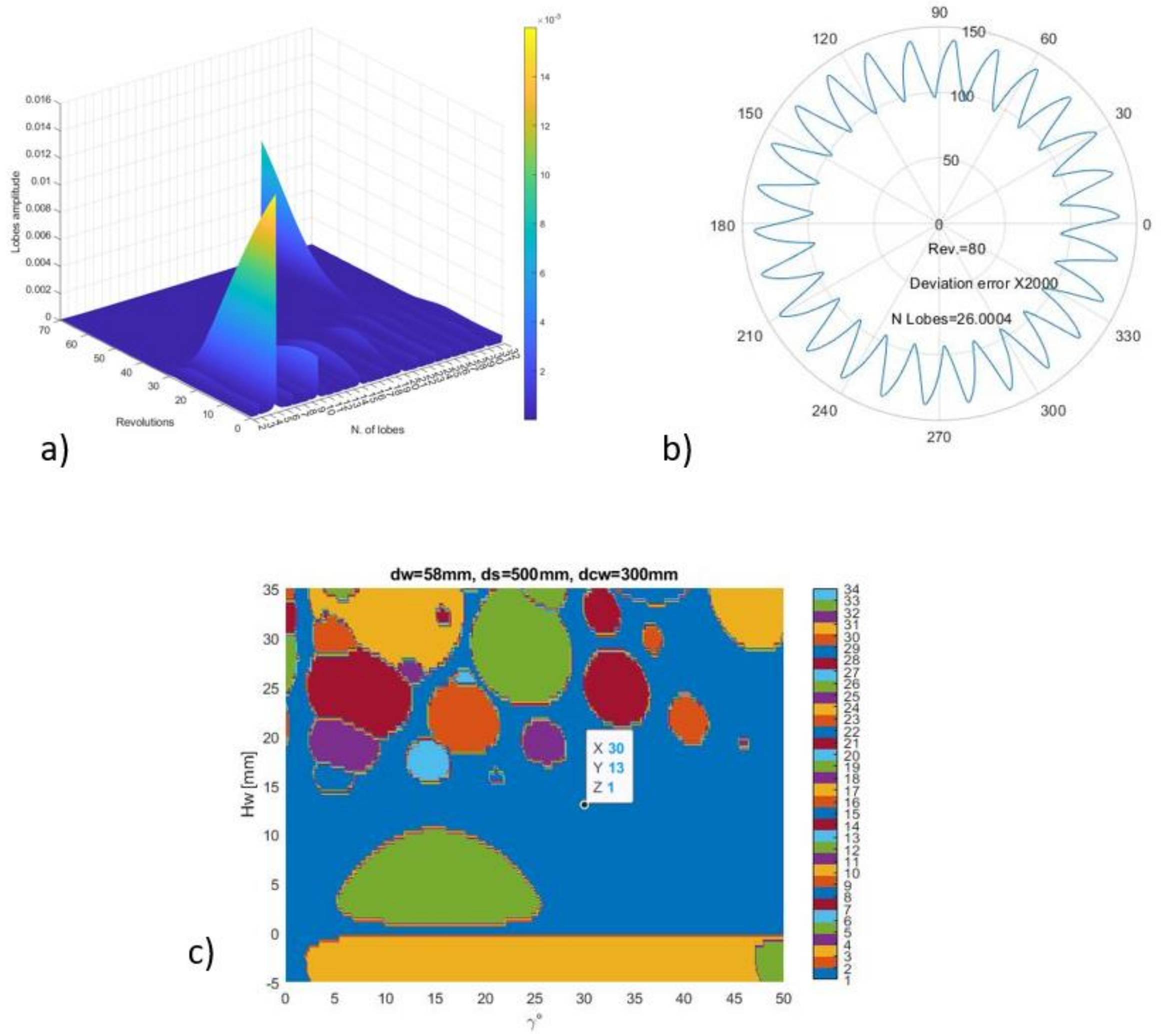

Figure 11: 5 lobed raw workpiece with Fixed Hw=13mm and Ɣ=30°, a) lobing development process, b) simulated final WP profile, c) geometric setup of the grinding

Figure 11depicts 5 lobed raw workpiece grinding process simulation, from Figure 11 (a) it can be seen that between 30 rev. and 40 rev. there is a transient zone that neither 5 lobes exist, nor 26 lobes are developed and for obtaining best results in terms of roundness the process should be terminated in that zone.

In next step same simulation is done based on conditions 2,3&4 and the results are presented by following figures. In each figure the results of two approaches (Continuous & multistep) are shown.

Figure 12 depicts the simulation done by varying both setup angles. As expected, the process has been initiated in a zone which develops 16 lobes profile and ends at a stable zone with Ɣ°=30° and β°=6.8°. From fig. 12.a and 12.b it is very clear that in continuous mode, once 5 lobed profile is reduced a 24 lobed profile is raised by with a very limited amplitude. But in multistep approach a similar behaviour like fixed angle approach was observed (Fig. 12.c & 12.d).

However, the simulations with other two approaches have reduced the difference between two methods (Continuous & multistep) in term of lobing development diagram (Figures 13.a, 13.c, 14.a, 14.c), but looking at simulated profiles (Figures 13.b, 13.d, 14.b, 14.d) it can be observed that the continuous method has produced smoother profile.

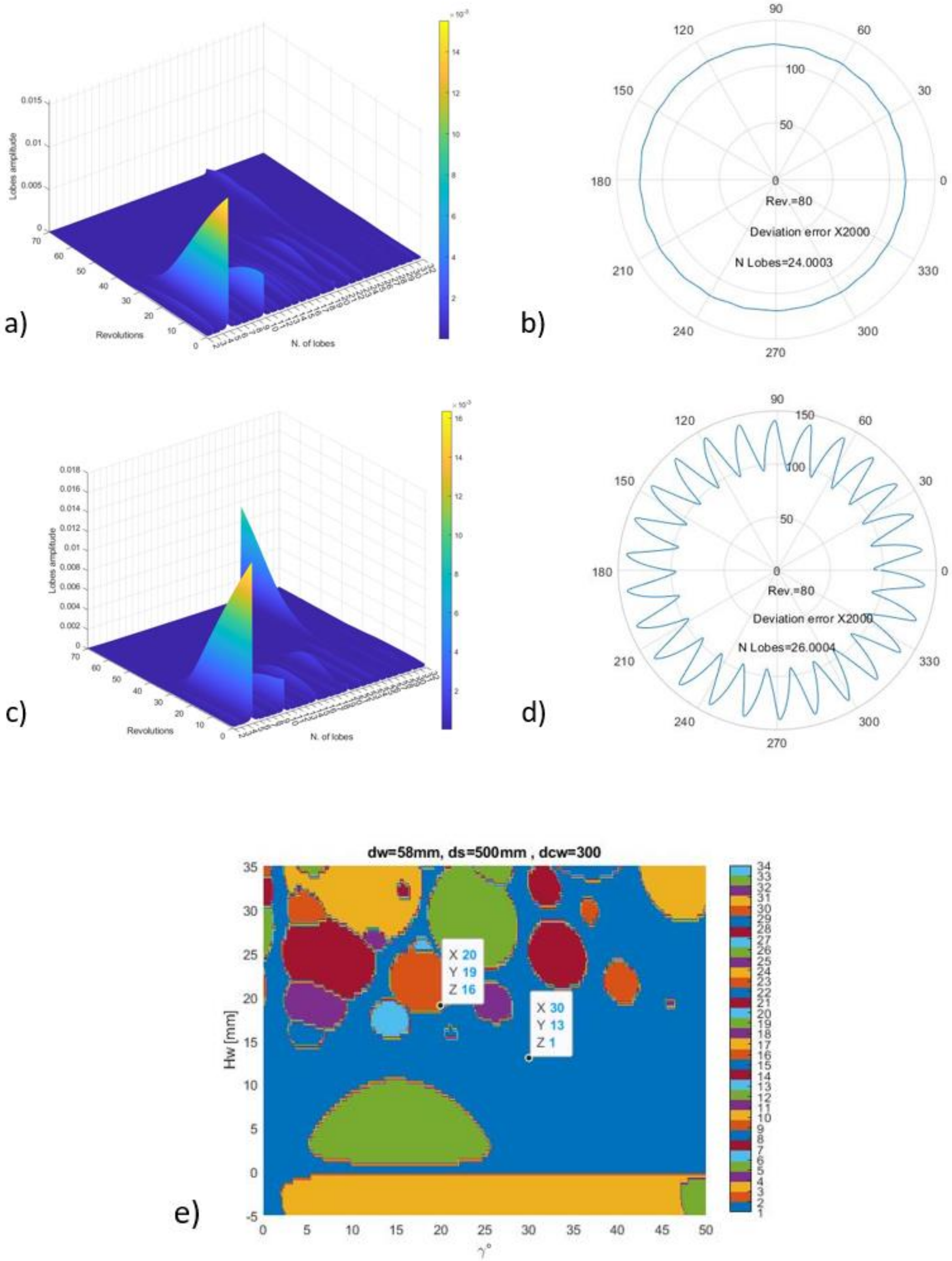

Figure 12: 5 lobed raw workpiece with varied both β° and Ɣ°, a) lobing development process (continuous), b) simulated final WP profile (continuous), c) lobing development process (multistep), d) simulated final WP profile (multistep s), e) Initial geometric set-up for grinding: Hw=19mm and Ɣ=20°, final: Hw=13mm and Ɣ=30°,

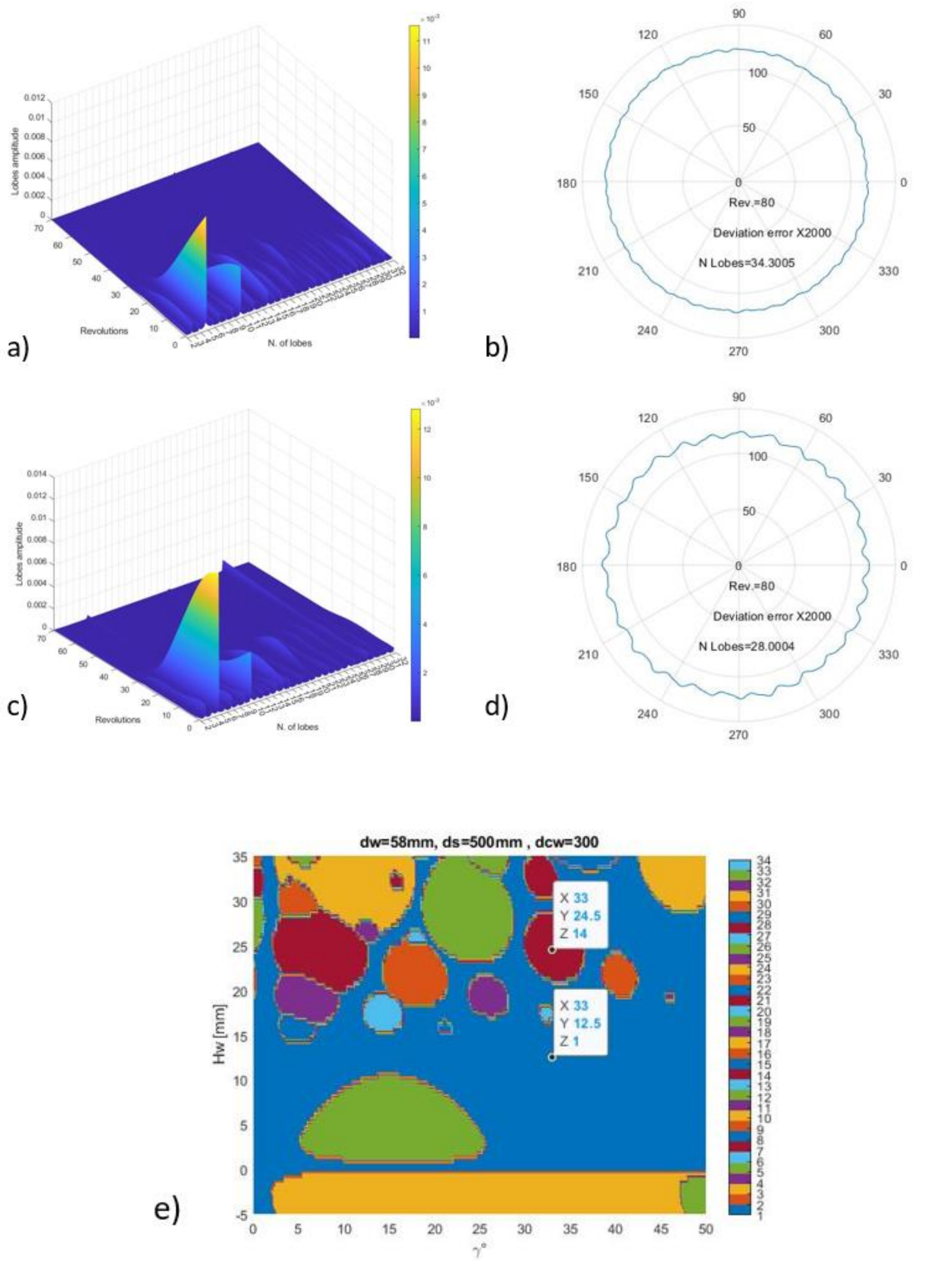

Figure 13: 5 lobed raw workpiece with varied β° with fixed Ɣ°, a) lobing development process (continuous), b) simulated final WP profile (continuous), c) lobing development process (multistep), d) simulated final WP profile (multistep s), e) geometric setup of the grinding initial: Hw=24.5mm and Ɣ=33°, final: Hw=12.5mm and Ɣ=33°,

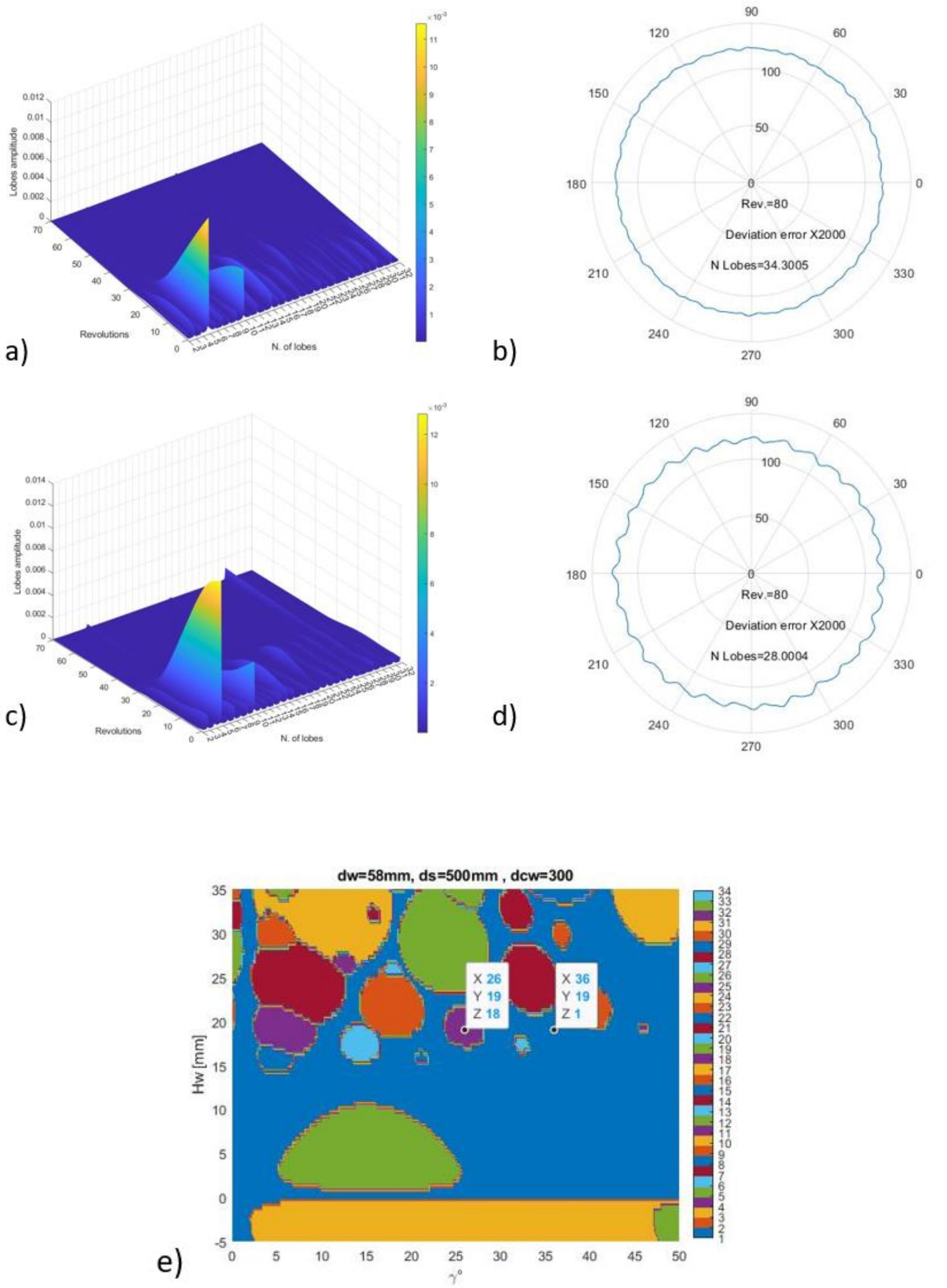

Figure 14: 5 lobed raw workpiece with fixed β° with varied Ɣ°, a) lobing development process (continuous), b) simulated final WP profile (continuous), c) lobing development process (multistep), d) simulated final WP profile (multistep s), e) geometric setup of the grinding initial: Hw=19mm and Ɣ=26°, final: Hw=19mm and Ɣ=36°,

Hence, looking comprehensively both simulated final WP profile and relative lobing development of the grinding process from *Figure 12* to *Figure 14* it can be seen clearly that in all 3 conditions the continuous variation of setup angles resulted in better final WP roundness and the best results was obtained with fixed β° (via Hw) and varied Ɣ°.

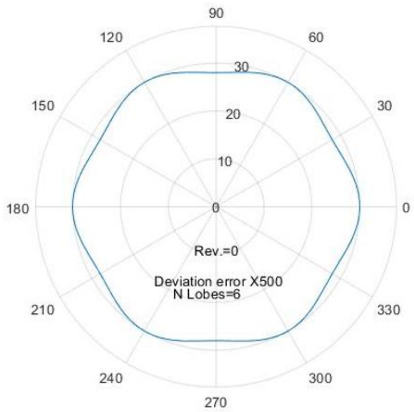

Figure 15: Raw workpiece with 6 lobes

As mentioned above the same simulations were done based on 6-lobed raw profile workpiece. The results of the classic fixed setup angles approach is comparable for those of 5-lobed WP. As *Figure 16* (a) shows the same transient zone exist in the lobing development graph and by passing that zone a 26 lobes profile is grown.

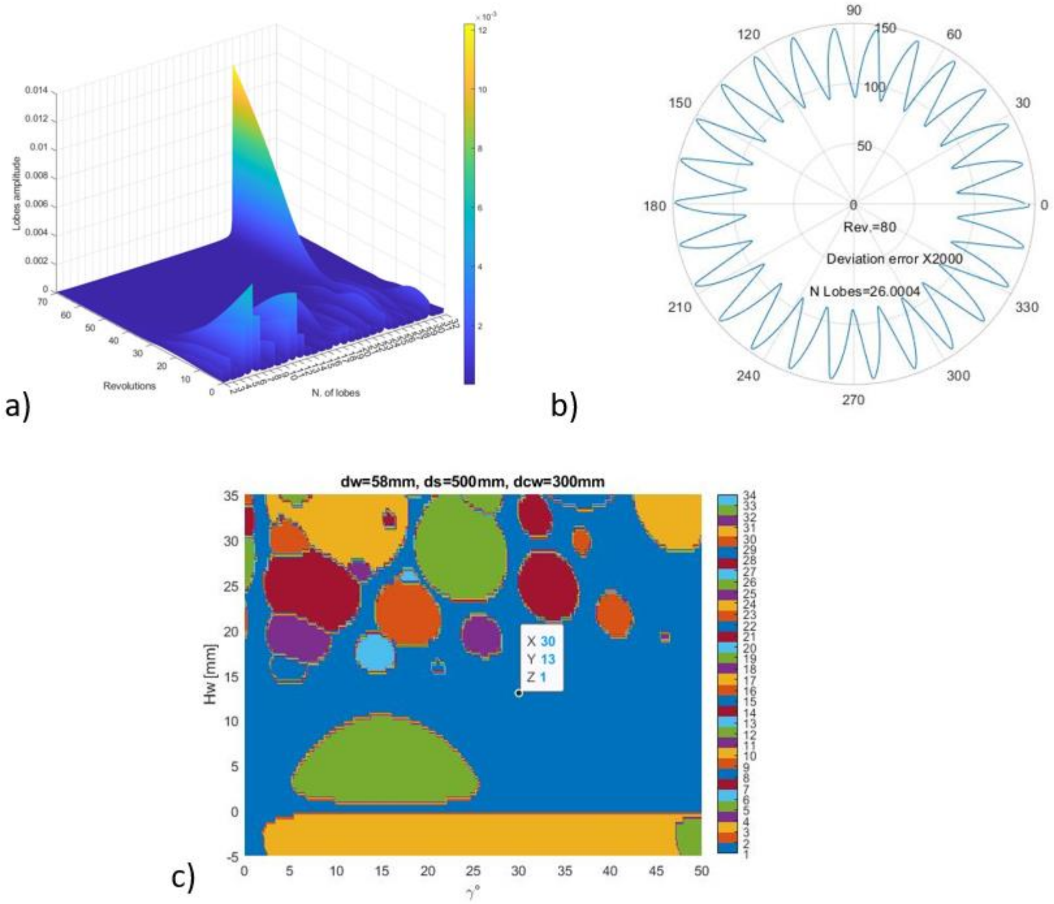

Figure 16. 6 lobed raw workpiece with Fixed Hw=13mm and Ɣ=30°, a) lobing development process, b) simulated final WP profile, c) geometric setup of the grinding

From *Figure 17* to *Figure 19* similar simulations as before are depicted for 6-lobed profile. As explained before, in this series of simulations, the initial point of grinding process is selected in a zone that encourages development of 5-lobes hopping that this condition accelerates the elimination process. The same as earlier approach, the process simulation is done considering a continuous change and a multistep change of setup angles. From these results it can be understood that similar to before the continuous variation method has the upper hand comparing to multistep method. And *Figure 19* presents that best roundness for even lobed raw profile can be achieved by continuous Ɣ° variation while the β° is fixed.

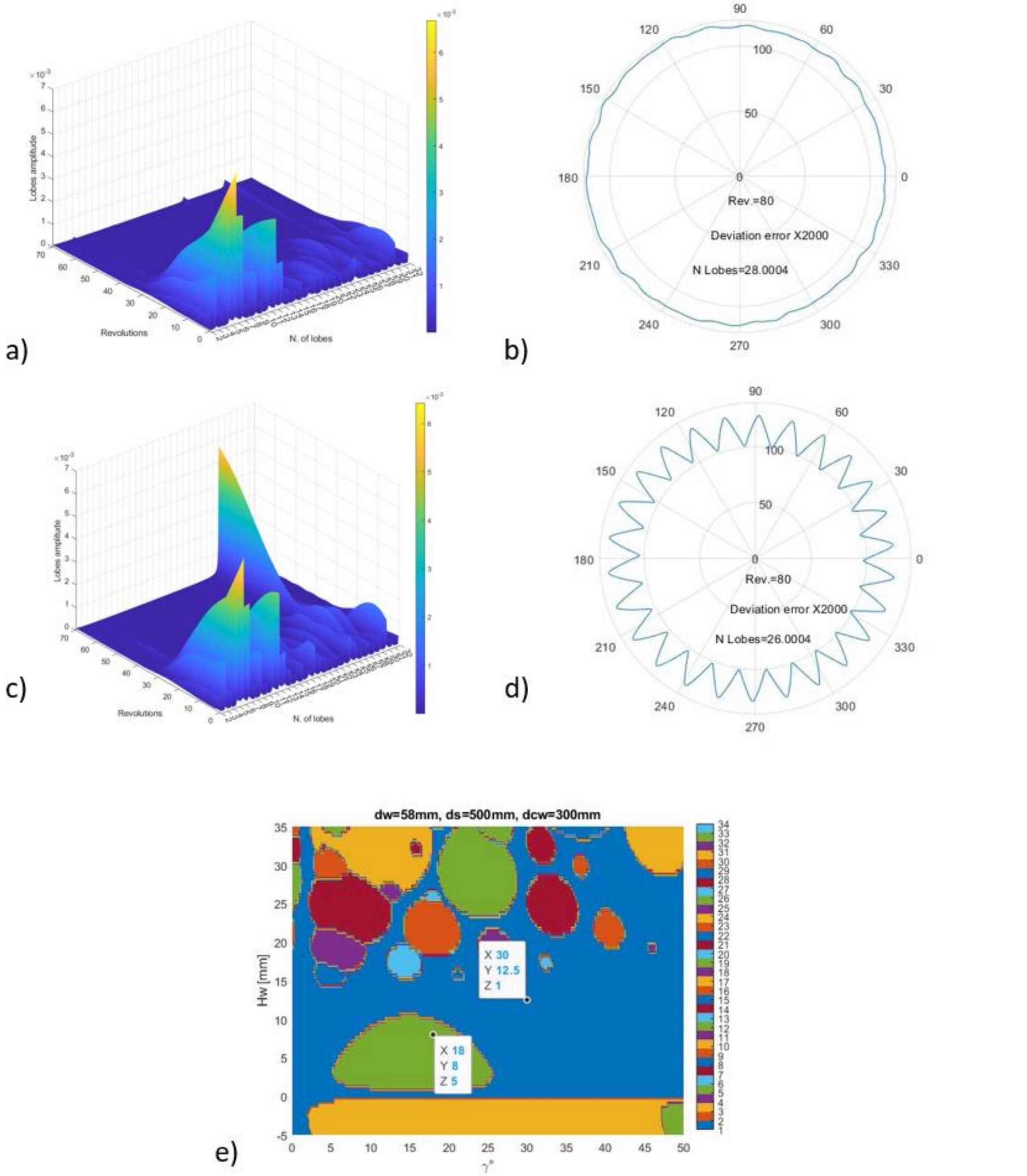

Figure 17: 5 lobed raw workpiece with varied both β° and Ɣ°, a) lobing development process (continuous), b) simulated final WP profile (continuous), c) lobing development process (multistep), d) simulated final WP profile (multistep s), e) geometric setup of the grinding initial: Hw=8mm and Ɣ=18°, final: Hw=12.5mm and Ɣ=30°,

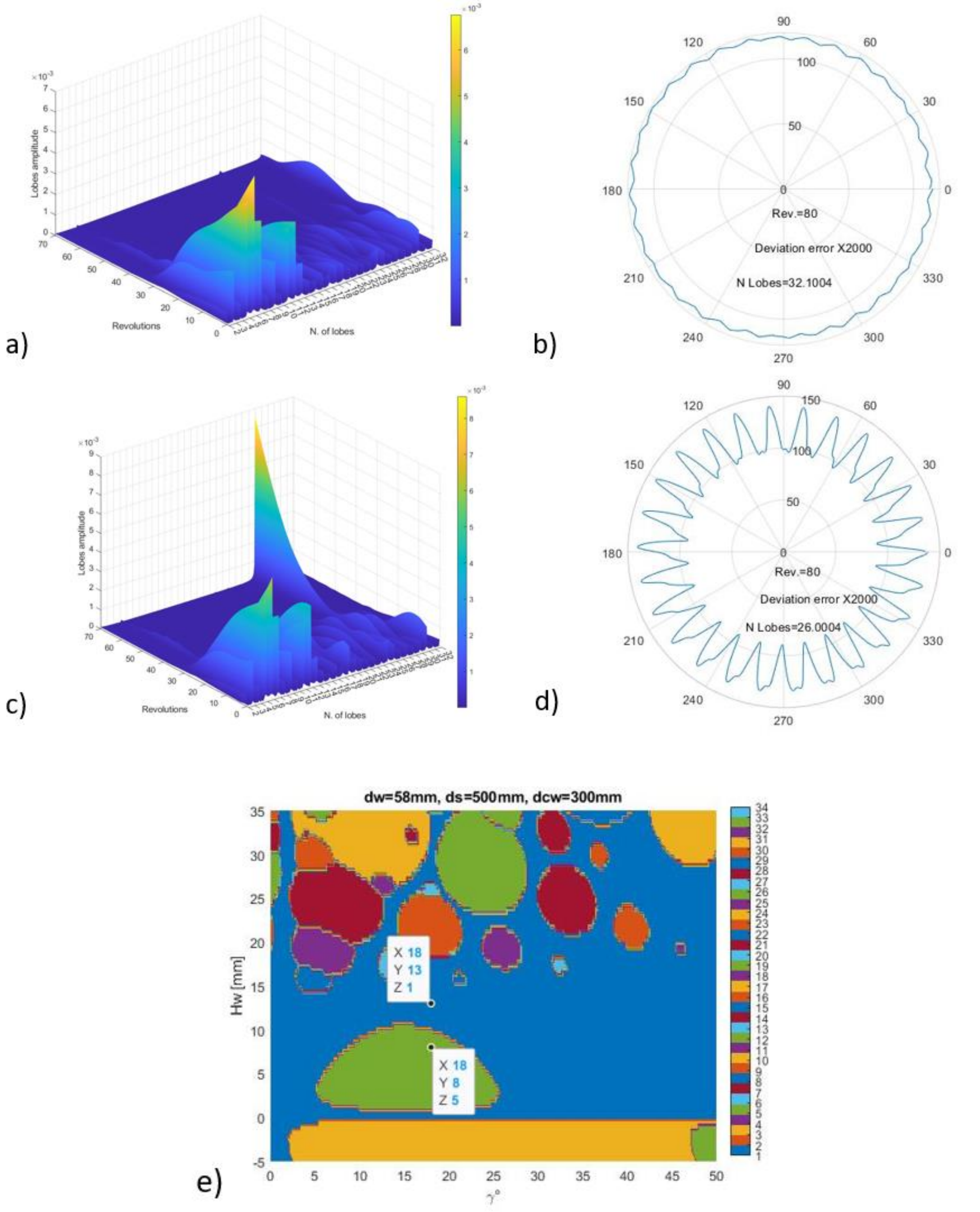

Figure 18: 6 lobed raw workpiece with varied β° with fixed Ɣ°, a) lobing development process (continuous), b) simulated final WP profile (continuous), c) lobing development process (multistep), d) simulated final WP profile (multistep), e) geometric setup of the grinding initial: Hw=8mm and Ɣ=18°, final: Hw=13mm and Ɣ=18°,

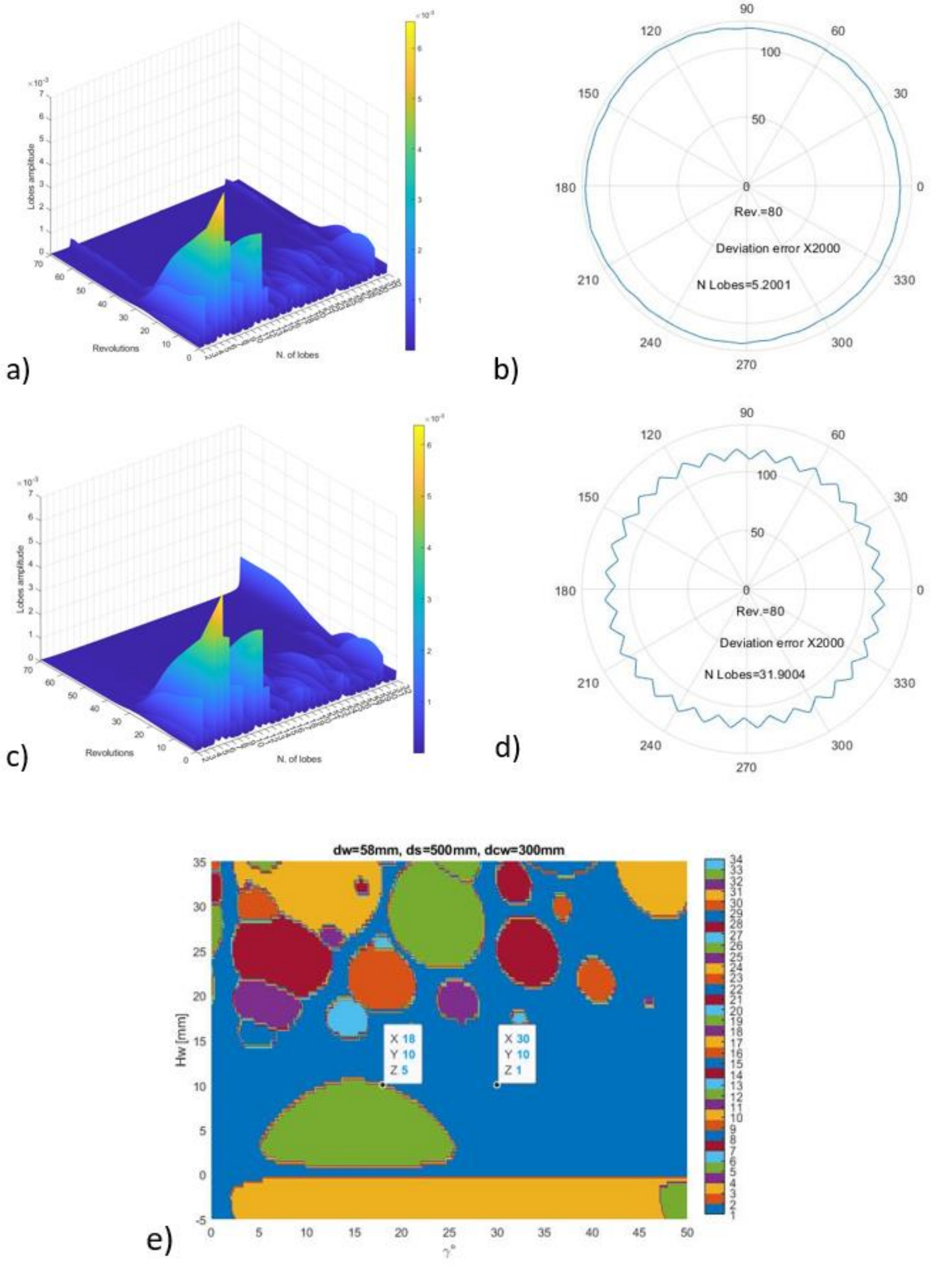

Figure 19: 6 lobed raw workpiece with fixed β° with varied Ɣ°, a) lobing development process (continuous), b) simulated final WP profile (continuous), c) lobing development process (multistep), d) simulated final WP profile (multistep s), e) geometric setup of the grinding initial: Hw=10mm and Ɣ=18°, final: Hw=10mm and Ɣ=30°,

5. Experimental verification

To validate the obtained model, a series of experimental tests were done. A highly non-round 3-lobe initial workpiece profile was selected (*Figure 21* a). The test has been executed on an industrial centerless grinding machine, with manual work rest blade adjustment (*Figure 20*) with few fixed parameters as reported in *Table 1*. The WP roundness has been measured with a "Mitutoyo Roundpack 400" system.

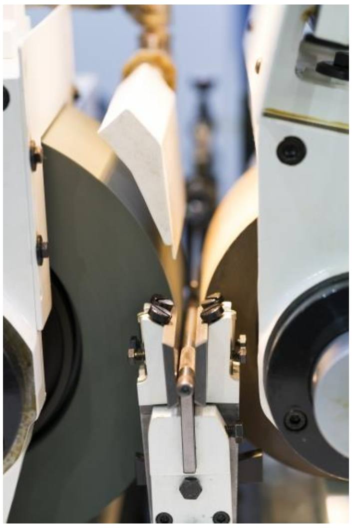

Figure 20. Centerless Grinding working zone

Table 1: DOE fixed parameters

	fixed parameters	*values*
1	Grinding Wheel linear velocity (Vs)	32 m/s
2	Regulating wheel diameter (nominal)	300mm
3	Operating wheel diameter (nominal)	500mm
4	Operating Wheel type (ANSI B74 13-1977)	500X165X254A 24A80L4V19
5	Regulating Wheel type (ANSI B74 13-1977)	300X157X127A 10A80RR
6	Workpiece material	C45
7	Workpiece diameter (WPD)	60 mm
8	Workpiece length	100 mm
9	Regulating wheel velocity	20 rpm
10	Feed rate	0.020 mm/sec

The first test was done with standard geometric setup (Ɣ=30°, h=13mm, β=6.8°) with 40 revolutions to stop the grinding process at the best condition as suggested in *Figure 11*. The second test was carried out by a support blade with Ɣ=30° but with two different heights (Hw1=24.5mm, Hw2=12.5mm) in entering and exiting work piece in a through feed grinding process with the same revolutions numbers as suggested in *Figure 13*.

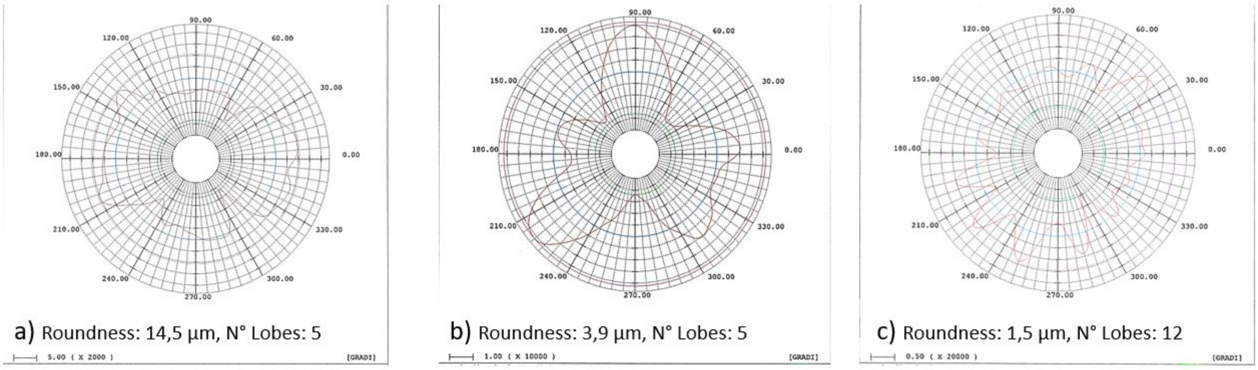

Figure 21: Experimental validation test results a) Raw workpiece, b) test with standard geometric setup, b) test with continuous β° variation.

The raw and the final ground workpieces' profiles are demonstrated in *Figure 21*. As it can be seen from *Figure 21*(b), after 40 revolutions of workpiece with fixed angles the roundness error is highly reduced from14.5µm to 3.8µm but the five lobed profile is persisted even though its amplitude is reduced. However, by looking at *Figure 21*(c), it can be observed that, the effect of continuous β° variation is very clear, the five lobed profile is completely eliminated and a new even lobing regime is created with much less amplitude with respect to before and the final roundness is arrived to 1.5µm with the same machine parameters and cycle time.

6. Discussion

As demonstrated the simulation results in section 4, it is very clear the importance of selecting right setup angles in a centreless grinding process. Traditionally the tangent angle β is set around 6°-8° for obtaining the best roundness mechanism, but this approach is working best with raw workpiece with high quality in terms of roundness and form error. Considering the situation in which the workpiece is defected by odd or even lobes from previous machining process the conventional method does not provide the best or fastest roundness correcting mechanism. So as presented above is the best to choose different approaches best on lobes already existed on the workpiece. It found that for elimination odd lobed profile the initial process should be start at a zone with even lobe encouraging behaviour and vice versa for the even lobed profile. This dual zone process can be done in continuous mode or in a multistage process, but even though the multistage method improved the rounding with respect to conventional method, but the best results is always obtained by continuous variation method.

Considering all 3 different combinations of two setup angle (β & Ɣ) to be fixed or varied different approaches can be chose based on type of grinding machine (plunge or through feed). In the plunge centreless grinding, the support blade is profiled base on different diameters presented on the workpiece therefore changing the Ɣ° continuously is not feasible and the only practical option can be changing the tangent angle β by changing the workpiece height.

On the other hand, in through feed process, the workpiece has a uniform diameter and Ɣ° can be changed continuously. Consequently, the support blade can be designed more freely to have a continuous change with the β° or Ɣ° or even both.

7. Conclusion

A new approach has been suggested to improve roundness mechanism of the centreless grinding based on classic stability diagrams and rounding mechanism already existed in the literature. The results presented in this paper indicate that it is not always convenient to keep setup angle fixed and based on raw workpiece roundness error changing continuously the setup angle from an initial appropriate point to a final point better results can be achieved. Furthermore, a new support blade design for through feed centreless grinding is presented for application of above-mentioned method.

Declarations

- Ethical Approval: The article follows the guidelines of the Committee on Publication Ethics (COPE) and involves no studies on human or animal subjects.
- Consent to Participate: Not applicable. The article involves no studies on humans.
- Consent to Publish: Not applicable. The article involves no studies on humans.
- Authors Contributions:
    - Hossein Safarzadeh: Conceptualization, Methodology, Software, Writing- Original draft preparation, Visualization, Validation, Investigation.
    - Michele Monno: Supervision and Reviewing.
- Competing Interests: The authors have no competing interests or conflicts of interest to declare that are relevant to the contents of this article.
- Availability of data and materials: The authors confirm that the data and material supporting the findings of this work are available upon request.

References

[1] M.. Dhavlikar, M.. Kulkarni, V. Mariappan, Combined Taguchi and dual response method for optimization of a centerless grinding operation, J. Mater. Process. Technol. 132 (2003) 90–94. https://doi.org/10.1016/S0924-0136(02)00271-6.

[2] S.S. Zhou, J.R. Gartner, T.D. Howes, On the Relationship between Setup Parameters and Lobing Behavior in Centerless Grinding, CIRP Ann. - Manuf. Technol. 45 (1996) 341–346. https://doi.org/10.1016/S0007-8506(07)63076-5.

[3] I. Gallego, Intelligent Centerless Grinding: Global Solution for Process Instabilities and Optimal Cycle Design, CIRP Ann. - Manuf. Technol. 56 (2007) 347–352. https://doi.org/10.1016/j.cirp.2007.05.080.

[4] F. Klocke, D. Friedrich, B. Linke, Z. Nachmani, Basics for In-Process Roundness Error Improvement by a Functional Workrest Blade, CIRP Ann. 53 (2004) 275–280. https://doi.org/10.1016/S0007-8506(07)60697-0.

[5] A. Dall, Rounding effect in centerless grinding, Mech. Eng. ASME. 58 (1946) 325–329.

[6] S. Yonetsu, Consideration of Centerless Grinding Characteristics Through Harmonic Analysis of Out-of-Roundness Curves, Proc. Fujihara Meml. Fac. Eng. Keio Univ. 12 (1959) 184–202.

[7] W.B. Rowe, M.M. Barash, Computer method for investigating the inherent accuracy of centreless grinding, Int. J. Mach. Tool Des. Res. 4 (1964) 91–116. https://doi.org/10.1016/0020-7357(64)90002-2.

[8] I.D. Marinescu, M.P. Hitchiner, E. Uhlmann, W.B. Rowe, I. Inasaki, Handbook of Machining with Grinding Wheels, CRC Press, 2006. https://doi.org/10.1201/9781420017649.

[9] R. Bueno, M. Zatarain, J.M. Aguinagalde, F. Le Maître, Geometric and Dynamic Stability in Centerless Grinding, CIRP Ann. - Manuf. Technol. 39 (1990) 395–398. https://doi.org/10.1016/S0007-8506(07)61081-6.

[10] W.B. Rowe, D.L. Richards, Geometric stability charts for the centerless grinding process, J. Mech. Eng. Sci. 14 (2016) 155–160.

[11] W.B. Rowe, M.M. Barash, F. Koenigsberger, Some roundness characteristics of centreless grinding, Int. J. Mach. Tool Des. Res. 5 (1965) 203–215. https://doi.org/10.1016/0020-7357(65)90011-9.

[12] Q. Cui, H. Ding, K. Cheng, An analytical investigation on the workpiece roundness generation and its perfection strategies in centreless grinding, Proc. Inst. Mech. Eng. Part B J. Eng. Manuf. 229 (2015) 409–420. https://doi.org/10.1177/0954405414530899.

[13] G. Bianchi, M. Leonesio, H. Safarzadeh, A double input describing function approach for stability analysis in centerless grinding under interrupted cut, Int. J. Adv. Manuf. Technol. (2020). https://doi.org/10.1007/s00170-020-05362-2.

[14] W.B. Rowe, Rounding and stability in centreless grinding, Int. J. Mach. Tools Manuf. 82–83 (2014) 1–10. https://doi.org/10.1016/j.ijmachtools.2014.03.004.

[15] M. Leonesio, J. Wojcicki, G. Bianchi, Geometrical optimization of centerless grinding process by profiled workrest, (2021) 3–8.

[16] H. Safarzadeh, M. Leonesio, G. Bianchi, M. Monno, Roundness prediction in centreless grinding using physics-enhanced machine learning techniques, Int. J. Adv. Manuf. Technol. (2020) 1051–1063. https://doi.org/10.1007/s00170-020-06407-2.

[17] W.B. Rowe, Principles of modern grinding technology, 2nd ed., Elsevier Inc, Oxford, 2009.